RSC Advances

PAPER

View Article Online
View Journal | View Issue

Cite this: *RSC Adv.*, 2025, **15**, 48

Preparation of a lanthanum-modified flocculant and its removal performance towards phosphorus and fluoride in yellow phosphorus wastewater†

Boxuan Li,[abc] Shaoxin Wen,[abc] Jiacheng Li,[abc] Dedong He,[abc] Yongming Luo,[abc] Xiangqian Zheng*[abcd] and Dingkai Chen *[abc]

Polysilicate-ferric-calcium-lanthanum (PSFCL) was synthesized through a co-polymerization method in order to treat the yellow phosphorus wastewater. Its morphology, composition and functional group were analyzed by X-ray Diffraction (XRD), Fourier Transform-Infrared Spectroscopy (FTIR), Scanning Electron Microscopic (SEM) and X-ray Photoelectron Spectroscopy (XPS), respectively. The optimization of the flocculant was also investigated, including La/Si molar ratio, pH, agitation time, dosage and sedimentation time. Results showed that PSFCL has reached an excellent removal efficiency of 95% and 97% towards phosphorus and fluoride, respectively. It could be inferred that charge neutralization, bridging effect and ligand exchange were the main coagulation mechanisms. As a whole, after the introduction of lanthanum, PSFCL was found to be a promising flocculant in yellow phosphorus wastewater treatment owing to its high removal efficiency and simple synthesis route.

Received 8th October 2024
Accepted 19th December 2024

DOI: 10.1039/d4ra07237e

rsc.li/rsc-advances

1. Introduction

In the past few decades, with the development of the chemical industry, a tremendous amount of phosphorus and fluoride have been produced and released into natural waterbodies *via* sewage discharge. The untreated wastewater can cause severe environmental issues. Excessive amounts of phosphorus can cause eutrophication problems which subsequently exacerbates the problem of algal bloom.[1] Moreover, excessive intake of fluoride by humans could be harmful to the oral system, skeleton, digestive systems, and other health issues.[2] Based on that, the aforementioned pollution problems have attracted much attention and become a worldwide environmental issue. Commonly used technologies towards phosphorus and fluoride removal include chemical precipitation,[3] coagulation,[4] adsorption,[5] advanced oxidation,[6] biological treatment,[7] membrane filtration,[8] *etc.* Among these treatment technologies, coagulation has been well adopted due to its cost-effective,[9] easy operation[10] and high removal efficiency.[11] Zhang *et al.*, applied a combined process of chemical precipitation and flocculation for TP removal. After adding calcium chloride, cPAM and adjusting pH value, the total removal efficiencies of TP and COD was 99%, 80%, respectively.[12] Macherzyński *et al.*, synthesized iron(II) sulfate(VI) and other pre-hydrolyzed coagulants for comparative studies of phosphorus removal, results showed that the iron coagulant (PIX-110) has reached a high phosphorus removal efficiency which is 99.5%.[13] Ozairi *et al.*, conducted a comparative study by using coagulation–flocculation process towards fluoride removal. The aluminum sulfate, polyaluminum chloride and ferric chloride were used for quantitative elimination of fluoride from wastewater. Results showed that the maximum removal efficiency of fluoride (83%) was obtained at 30 mg L^{-1} of aluminum sulfate.[14]

At present, the most widely used coagulants contain conventional aluminum or iron salt, poly-aluminum chloride (PAC),[15] poly-ferric sulfate (PFS),[16] and poly-ferric chloride (PFC).[17] Nevertheless, the residual coagulants are harmful to the human nervous system, and ferric and aluminum ions can cause secondary pollution problems which may need further treatment processes and more capital investment.[18] Based on the above situation, polyciliate composite flocculants were developed in order to solve these problems. Polysilicate is an anionic flocculant which does not show great health risk. A polysilicate composite flocculant combines the stability of polysilicate and the high-efficiency flocculation ability of metal salts. Compared with the low molecular weight and traditional high molecular weight inorganic flocculants, polysilicate composite metal salt flocculants show excellent removal performance, including higher average molecular weight and enhanced effect in charge neutralization, adsorption and

[a]*Faculty of Chemical Engineering, Kunming University of Science and Technology, Kunming 650500, P. R. China. E-mail: 371249656@qq.com; cdk684983@163.com*
[b]*The Innovation Team for Volatile Organic Compounds Pollutants Control and Resource Utilization of Yunnan Province, Kunming 650500, P. R. China*
[c]*The Higher Educational Key Laboratory for Odorous Volatile Organic Compounds Pollutants Control of Yunnan Province, Kunming 650500, P. R. China*
[d]*Institute for Inspection and Certification of Xishuangbanna Dai Autonomous Prefecture, Jinghong 666100, P. R. China*

† Electronic supplementary information (ESI) available. See DOI: https://doi.org/10.1039/d4ra07237e

bridging effect.[19] Liu *et al.* synthesized a high molecular polysilicate composite flocculant by adding metal magnesium salt and silicate into the traditional PAC, the results showed that its decolourization efficiency is more than 90% which is better than other traditional coagulants.[20] Liu *et al.* investigated an alginate grafted polysilicate aluminum calcium in drinking water treatment, the introduction of alginate and calcium has greatly enhanced the turbidity removal efficiency and color removal efficiency to 97% and 98%, respectively.[21] Wu *et al.* synthesized a polysilicate aluminum ferric (PSAF) for oil wastewater treating. The results indicated that when the (Al + Fe)/Si ratio was 6 : 4 and Al/Fe ratio was 5 : 5, the PSAF reached a prefect turbidity removal rate and oil removal rate of 99%, 88%, respectively.[22] All of the above results have shown the great potential of polysilicate composite metal salts in practical application.

In this study, a polysilicate composite flocculant was synthesized *via* co-polymerization to measure its performance towards yellow phosphorus wastewater. After the polysilicate was prepared, the polysilicate doped with ferric (PSF), ferric-calcium (PSFC) and ferric-calcium-lanthanum (PSFCL) were added to the wastewater to remove the phosphorus and fluoride, respectively. Besides, its removal performance was also optimized by adjusting pH and SiO_2 content of polysilicate, La/Si molar ratio, agitation time, pH, dose and sedimentation time. This study could provide a new perspective for the removal of phosphorus and fluoride from wastewater by coagulation and optimization of the reaction conditions for further practical application.

2. Material and methods

2.1 Materials

Sodium silicate ($Na_2SiO_3 \cdot 9H_2O$), lanthanum nitrate hexahydrate ($La(NO_3)_2 \cdot 6H_2O$), and ferric chloride hexahydrate ($FeCl_3 \cdot 6H_2O$) were purchased from Zhiyuan Chemical Reagent Co., Ltd (Tianjin, China), calcium nitrate tetrahydrate ($Ca(NO_3)_2 \cdot 4H_2O$) was purchased from Shanghai Aladdin Chemistry Co., Ltd (Shanghai, China). Hydrochloric acid (36%) was provided by Kelong Chemical Co., Ltd (Chengdu, China). Ultrapure water (R = 18.3 MΩ cm^{-1}) was used for all the experiments. Yellow phosphorus wastewater was collected from a local yellow phosphorus chemical plant in Kunming, the characteristics were shown in Table 1. All of these reagents were analytical reagent without further purification.

2.2 Preparation of flocculants

Flocculants were prepared as the following procedure at room temperature. Firstly, sodium silicate solution was dropwise added to the hydrochloric acid to polymerize and form polysilicic acid solution (PSI). To ensure an ideal degree of PSI polymerization, several pre-experiments were carried out, the pH was adjusted with 36 wt% (1 + 1) hydrochloric acid. As shown in Fig. S1 and S2,†the pH and silica content can significantly affect the polymerization time, an extremely short polymerization time could inhibit the metal salts bonding with PSI. However, when the polymerization time is too long, the PSI preparation process will be prolonged and consequently affect the degree of polymerization. In a word, the optimal pH of synthesized PSI and silica content was determined to be 2 and 2%, respectively. The obtained solution was then agitated for two hours to form PSI. A certain amount of ferric chloride hexahydrate $FeCl_3 \cdot 6H_2O$, calcium nitrate tetrahydrate $Ca(NO_3)_2 \cdot 4H_2O$ and lanthanum nitrate hexahydrate $La(NO_3)_2 \cdot 6H_2O$ solution were slowly added into the PSI independently under constant magnetic stirring for 1 hour to form PSF, PSFC and PSFCL. The polysilicate-ferric-calcium-lanthanum (PSFCL) flocculant was obtained by agitating for another 12 h. PSF and PSFC could be obtained *via* adding ferric salt, calcium lanthanum salt, respectively. After 12 h continuously agitation, the formation of solid-state flocculants was achieved.

2.3 Coagulation experiments

The coagulation experiments were carried out in several plexiglass beakers using a magnetic stirrer *via* a 3-step procedure, *i.e.*, high rate stirring, coagulation and sedimentation. The wastewater was diluted 20 times before the experiments were conducted. In the high rate stirring step, the stirring rate was set in 200 rpm, the dose of each experiment was 6 ml/200 ml, and the pH of each solution was maintained at 5 by using hydrochloric acid and sodium hydroxide. The aliquots were extracted by syringes and then filtered through a 0.45 μm filter. In the end, the zeta potential of each flocs was measured. In the coagulation step, the stirring rate was decreased to 60 rpm for 5 min before the sedimentation step. All of aliquots were taken below 2–3 cm of the surface after 30 min sedimentation for phosphorus, fluoride, and turbidity test. The removal percent (R%) for turbidity, phosphorus and fluoride was calculated by eqn (1).

$$R\% = \frac{C_0 - C_e}{C_0} \times 100\% \quad (1)$$

in the equation above, C_0 stands for initial concentration of phosphorus or fluoride, C_e stands for the concentration of phosphorus or fluoride at equilibrium and R% stands for removal efficiency.

2.4 Characterizations of flocculants

The residue concentration of phosphorus present in the solution was measured by molybdenum blue spectrophotometric

Table 1 Characteristics of yellow phosphorus wastewater

COD (mg L^{-1})	TSS (mg L^{-1})	Turbidity (NTU)	TF (mg L^{-1})	TP (mg L^{-1})	pH	Zeta potential (mV)
61	545	10	103	3268	2.1	−24.45

method *via* a UV spectrophotometer (723PC, China). The concentration of fluoride was determined by a fluorine ion meter (DWS-51, China). The solid samples of the flocculants were analyzed by Fourier transform infrared spectroscopy (FT-IR) with the Thermos Scientific Nicolet Is-50 spectrometer in the range of 4000–400 cm^{-1}. X-ray diffraction (XRD) was measured by XRDynamic 500 (Anton Paar, Austria) for the determination of crystalline with Cu Kalpha radiation in the 2θ range of 20–80° at a scan rate of 4° min^{-1}. The microstructure of flocculants and elemental compositions was examined by a Scanning Electron Microscope (SEM) (Zeiss Sigma 300, Germany). The XPS spectra were analyzed using X-ray photoelectron spectroscopy (Thermos Scientific K-Alpha, USA) with Al Kα radiation (hv = 1486.6 eV). Zeta potential for wastewater samples and flocculants was obtained by a nanoparticle size and zeta potential analyzer (Anton Paar Litesizer 500, Austria). The pH values and turbidity of solutions were measured by a pH meter (PHS-3C, China) and a turbidimeter (WGZ-200BS, China). Data processing was conducted *via* Origin 2021 software.

2.5 Statistical analysis

One-way analysis of variance (ANOVA) with Fisher's least significant difference (LSD) post hoc (α – 0.05) tests was used to determine the significant differences in investigated pollutants removal from phosphorus and fluoride using different molar ratio; pH values; dosages; agitation time and sedimentation time. All calculations were carried out using Origin 2021 software.

3. Results and discussion

3.1 Morphology and structure

3.1.1 SEM-EDS analysis. The SEM photographs of PSF, PSFC and PSFCL were conducted in Fig. 1. Fig. 1a showed that PSF had a relatively smooth surface and scattered particles, indicating that its bridge ability is inferior. PSFC had a rough brick-shaped structure, as shown in Fig. 1b, demonstrating this sample has a trend of agglomeration. Fig. 1c exhibited a dispersed and porous skeleton structure of PSFCL since the introduction of several metal salts roughens the surface and enriches the multi-branch system compared with PSF and PSFC to form a dense polymer composite.[23] The SEM image of PSFCL indicated that it possesses a relatively high specific surface area and dense structure, which significantly enhance the ability of adsorption, complexation and bridging. In the end, SEM photograph of PSFCL after coagulation was shown in Fig. 1d. The flocs exhibited a rough surface covered with irregular branched chain structure, implying the occurrence of adsorption and flocculation process. The branched chain structure promoted the charge neutralization, adsorption and bridging, which was conducive to the colloidal particle formation and subsequent settlement.[24]

The distribution of PSFCL elements after coagulation was determined by EDS, and specific atomic percentage and corresponding elements distribution were shown in Fig. S3.† The result showed that each element was uniformly dispersed, and phosphorus and fluoride were successfully loaded after coagulation process.

3.1.2 XRD analysis. Fig. 2a illustrated the XRD spectra of PSF, PSFC and PSFCL, and the results showed that these XRD patterns were similar and almost identical. It could be seen that $Fe(OH)_3$, Fe_2O_3, Fe_3O_4, SiO_2, $Ca(OH)_2$, CaO and other diffractive peaks could not be observed, which indicated that the synthesized flocculant was a complicated polymer including ferric, silicon, calcium and lanthanum, rather than a simply physical mixture of metal salts. The calcium, iron, lanthanum, silicon and other elements in the flocculant had been polymerized in an amorphous form without standard diffractive crystals

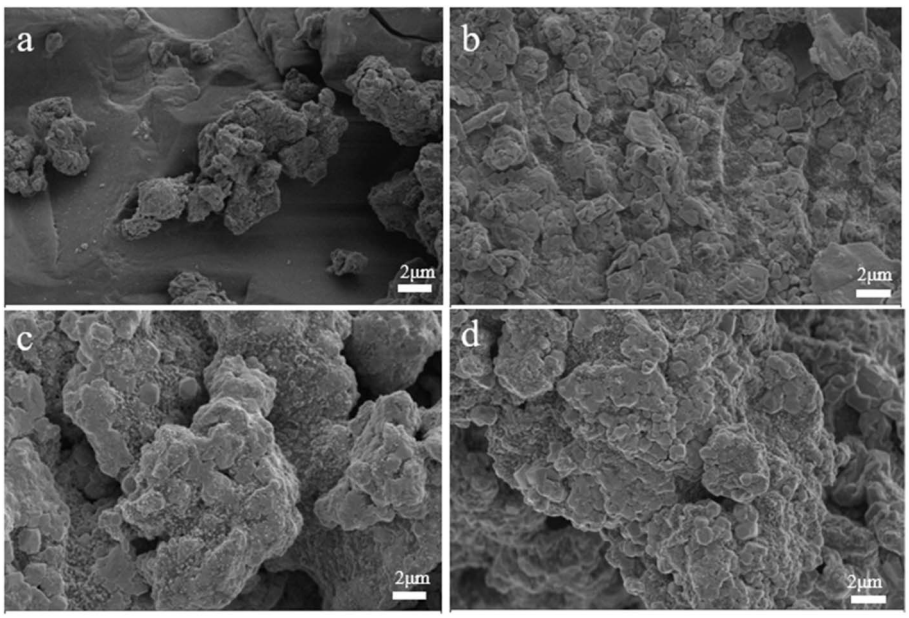

Fig. 1 SEM images of PSF (a); PSFC (b); PSFCL (c); PSFCL after coagulation (d).

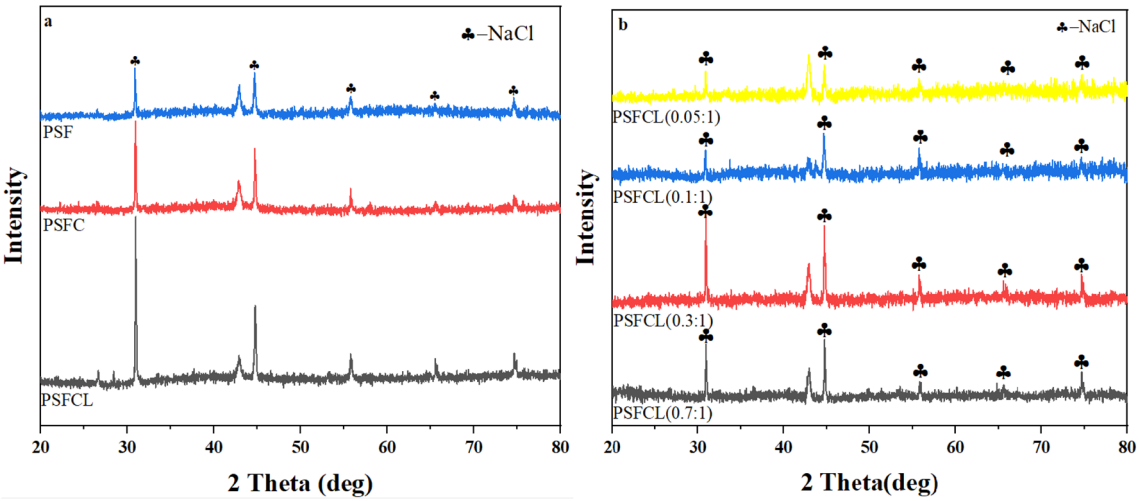

Fig. 2 (a) XRD spectra of PSF, PSFC and PSFCL; (b) XRD spectra of PSFCL under different La/Si molecular ratio after flocculation.

spectra. The strong diffractive peaks at 32° and 46° were assigned to NaCl, which was a by-product formed *via* dehydration process of samples.[11]

The XRD pattern of PSFCL under different La/Si molecular ratio after flocculation was shown in Fig. 2b. The result indicated that after flocculation there was almost no crystal phase difference between each flocculant, and the peak strength for each flocculant with different La/Si ratio was fluctuant. Moreover, with the increase of the La/Si ratio, the crystal phases of each flocculant seem be identical compared with PSFCL pattern in Fig. 2a, which guarantee an excellent stability of the flocculant. Polysilicate with excellent charge neutralization and adsorption bridging abilities is a promising coagulation agent.[25] The introduction of polysilicic acid has large particle size and molecular weight which leads to strong adsorption bridging effect.[26] In a word, polysilicate can act as skeleton materials and form hydrophobic channels to improve wastewater coagulation performance. If macromolecular substances were dominant in the composition of coagulants, the coagulation efficiency towards target pollutant was usually higher. The macromolecular substances could stimulate the bridge effect which was conductive for the formation of flocs, and these flocs could be easily settled for the subsequent separation.[27]

3.2 Evaluation of coagulation performance

3.2.1 Effect of La/Si molar ratio. The La/Si molar ratio was investigated to determine the optimal coagulation performance and degree of polymerization, as shown in Fig. 3a. The coagulant performance was varied by adjusting the La/Si molar ratio. When lanthanum was absent within the flocculant, the removal efficiency towards phosphorus was 90%. The removal efficiency continuously increased to 96% as the La/Si molar ratio increased to 0.1. When La/Si molar ratio was over 0.1, the removal efficiency was stabilized around 98%. The trend was similar to that of fluoride removal. With the increase of La content, the removal efficiency towards fluoride increased from 60% to 91% when the La/Si molar ratio reached 0.3. In order to ensure an excellent coagulation performance for both phosphorus and fluoride, the La/Si molar ratio of 0.3 was chosen as the optimal molar ratio.

3.2.2 Effect of pH. It had been confirmed that the pH of solution had a great influence in removal efficiency of phosphorus.[28] In this study, the residual phosphorus and fluoride content was tested at pH = 1–10 as shown in Fig. 3b. The composite coagulant had its worst performance when the solution was in extreme acidic or alkaline condition. In extreme acid condition, H^+ ions would compete with positively charged metal ions to bond with anionic colloids and subsequently weakened the effect of charge neutralization. Moreover, excess H^+ ions in the solution would consume the OH^- and inhibited the hydrolysis process during the coagulation.[29] When the pH increased, the removal efficiency of phosphorus continuously enhanced and reached to the plateau of 97% at pH = 5. The flocculant hydrolyzed to produce a large number of high valence polynuclear hydroxyl complex ions. These ions were adsorbed on the surface of negatively charged particles, leading to amplify the charge neutralization process.[30] In alkaline condition, the hydrolysis process of metal ions was accelerated *via* reaction with excess OH^- in the solution which leaded to occurrence of precipitation. When pH was in the range of 7–11, the net-shaped structure of polysilicic acid was partially destroyed due to the breakage of Si–O–Si bond, subsequently weakening the bridging effect of the coagulant towards phosphorus and fluoride. Compared with the removal efficiency of phosphorus, that of fluoride could maintain a good performance in both acidic and neutral condition. When pH was 3, the maximum fluoride removal efficiency reached 98%. When pH was over 7, the negatively charged fluorine atoms could bond with positively charged hydrogen atoms to form hydrofluoric acid which could dissolve in alkali environment, leading to unsatisfied removal efficiency. Therefore, in order to achieve an optimal removal performance for phosphorus and fluoride, the solution pH was set to 5 for all the coagulation experiments.

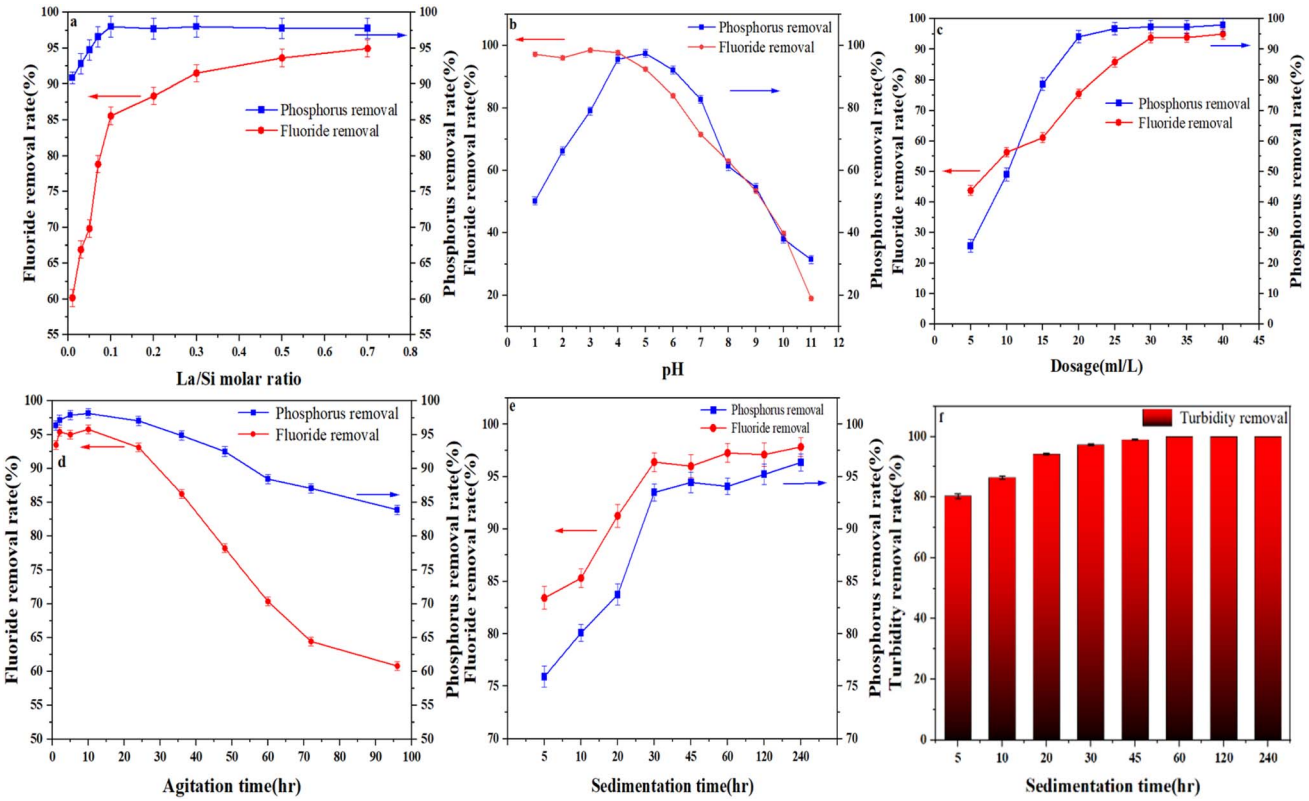

Fig. 3 Effect of (a) La/Si molar ratio; (b) pH; (c) dosage; (d) agitation time; (e) sedimentation time towards the removal of phosphorous and fluoride; (f) effect of sedimentation time towards the removal of turbidity.

3.2.3 Effect of dosage. Fig. 3c illustrated the effect of dosage on phosphorus and fluoride removal performance. When the dosage was 1 ml, the removal efficiency of phosphorus and fluoride was the lowest level which was 25% and 43%, respectively. With the increase of the dosage, the removal efficiency significantly enhanced and reached the highest level when the dosage was around 6 ml, subsequently maintaining stable. Once the coagulant was released into water body, it would hydrolyze immediately and bond with the anionic ions *via* charge neutralization. However, excessive amount of coagulant would cover the surface of metal particles, leading to "ion binding" effect, which significantly reduced the aggregation of suspended particles and coagulation performance.[31] Additionally, the excess amount of flocculant would lead to charge reversal of metal particles, which could also reduce the removal performance towards phosphorus and fluoride.[32]

3.2.4 Effect of agitation time. An appropriate agitation time was crucial to the degree of polymerization. In this study, we investigated the effect of agitation time towards phosphorus and fluoride removal, the agitation time was set to 1–96 hours as shown in Fig. 3d. Result showed that when the agitation time was below 24 hours, the flocculant remained high removal efficiency which was over 93% for phosphorus and fluoride. When the agitation time reaches 10 hours, the phosphorus and fluoride removal efficiencies have reached to the plateau which is 98% and 96%, respectively. Afterthe agitation time exceeded 36 hours, the removal efficiency gradually decreased, which was mainly caused by the decreasing stability of composite flocculant, leading to the weakening of bridging effect. As a whole, in order to guarantee a good removal performance, the optimal agitation time was supposed to be 10 hours.

3.2.5 Effect of sedimentation time. The effect of sedimentation time towards phosphorus and fluoride removal was shown in Fig. 3e. The optimal sedimentation time test was set to 5–120 min. The result showed that limited sedimentation time was not adequate for suspended particles to settle down, resulting in poor removal efficiency. When the sedimentation time increased from 5 to 30 min, the removal efficiency enhanced significantly, reaching to 96% and 93%, respectively, for phosphorus and fluoride. Due to the high molecular weight of PSFCL, it could effectively generate large numbers of big flocs to sweep most of the small particles *via* bridging effect during the coagulation process. To ensure an excellent coagulant performance, the sedimentation time was set to 30 min. Under the optimal conditions, the turbidity removal test was conducted, and the result was shown in Fig. 3f. The result indicated that the turbidity removal rate continuously increased from 80% to almost 99% when the sedimentation time reached 45 min. In summary, PSFCL displayed an excellent turbidity removal efficiency.

3.3 Comparison of the removal efficiencies of various flocculants

The removal efficiency of PSF, PSFC and PSFCL in the diluted yellow phosphorus wastewater was investigated, as shown in

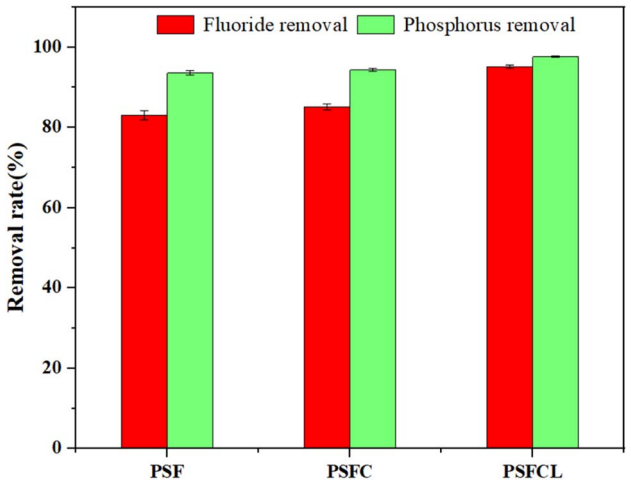

Fig. 4 Comparison of removal efficiency of three flocculants under optimized conditions (La/Si molar ratio = 0.3, pH = 5, dosage = 30 ml L^{-1}, agitation time = 10 h, sedimentation time = 30 min).

Fig. 4. Each flocculant at identical dosages (PSF: 30 ml L^{-1}, PSFC: 30 ml L^{-1}, PSFCL: 30 ml L^{-1}) was added into yellow phosphorus wastewater sample at room temperature (25 °C). After the introduction of lanthanum, the removal efficiency of the composite flocculant PSFCL significantly enhanced compared with that of PSF and PSFC, with the phosphorus and fluoride removal efficiency of 97% and 95%, respectively. Compared with other reported flocculants in Table 2, PSFCL has shown great performance towards simultaneously phosphorus and fluoride removal.

3.4 Flocculation mechanism

3.4.1 FTIR analysis. The FTIR spectra of PSF, PSFC and PSFCL in Fig. 5a demonstrated the presence of the strong absorption peak at 3000–3600 cm^{-1}, assigned to the stretching vibration of –OH group.[36] The wide absorption peak indicated a relatively large amount of –OH group in the flocculant. It was speculated that the –OH group may originate from the stretching vibration of complexation between ferric-silica, and –OH was from the coordinated water in polysilicic acid and adsorbed water molecules within the samples. The absorption peaks at 1615 cm^{-1} and 1618 cm^{-1} were relevant to the bending vibration of adsorbed water molecules, coordinated water and crystal water molecules.[11] The peak at 1093 cm^{-1} was assigned to the stretching vibration of Si–O–Fe, which may derive from the complexation between polysilicic acid and ferric ions or Fe–OH group.[19] The peak at 668 cm^{-1} was attributed to the vibration of Fe–OH or Si–OH group. The peak at 457 cm^{-1} was owe to the stretching vibration of Fe–O group.[37] Compared with PSF and PSFC, there were two new absorption peaks presented in PSFCL. The absorption peak at 1446 cm^{-1} was assigned to the stretching vibration of La–O–La band.[38] The absorption peak at 742 cm^{-1} was ascribed to Si–O–La. These two peaks indicated that lanthanum could bond with fluoride *via* complexation, which was conducive to the removal of fluoride within wastewater. The above results demonstrated that the PSFCL was not a simple physical mixture of metal salt and polysilicate, which was correspondent to the previous XRD result. As a whole, it could be inferred that lanthanum, polysilicic acid, ferric and calcium underwent a complicated chemical reaction and formed a new inorganic polymer composite.

Fig. 5b showed the comparison of PSFCL spectra before and after flocculation. The characteristic peaks at 1073 cm^{-1} and 812 cm^{-1} were assigned to the bending vibration of Si–O–Si and Si–O–Fe, respectively. After coagulation, the band at 3388 cm^{-1} shifted to a higher frequency at 3452 cm^{-1}, this indicated that –OH group interacted with fluorine ions which was conductive to removal of fluoride and phosphorus. The broadband at 1000–1100 cm^{-1} corresponded to P–O stretching vibration, which demonstrated a successful load of phosphorus on PSFCL. Moreover, the peaks at 1060 cm^{-1}, 668 cm^{-1} and 457 cm^{-1} disappeared, which indicated that La and Fe were involved in the coagulation process. The absorption peak at 467 cm^{-1} and 550 cm^{-1} after adsorption demonstrated that the metal interacted with fluorine ions *via* complexation to form M–F bonds (M = La or Fe).[39]

3.4.2 Zeta potential. To better understand the electrostatic interaction and coagulation mechanism during the coagulation process, the zeta potential of raw wastewater, PSF, PSFC and PSFCL was measured as shown in Fig. 6. The zeta potential in PSF, PSFC and PSFCL was 20.42 mV, 4.87 mV and 5.93 mV, respectively. This indicated that these flocculants were all positively charged and capable of bonding with negatively particles within raw wastewater *via* charge neutralization.

Table 2 Coagulation capacities of phosphorus and fluoride on metal-based flocculants[a]

Samples	pH	Dose (mg L^{-1})	Stir rapidly	Stir slowly	Settling time (min)	TP removal rate (%)	TF removal rate (%)	Ref.
PFASiC	5–9	50	150 rpm, 3 min	30 rpm, 10 min	30	>95	—	33
PAC	6–8	50	150 rpm, 3 min	30 rpm, 10 min	30	94	—	33
$ZrCl_4$	4–6	24	200 rpm, 1 min	40 rpm, 15 min	20	—	85	34
$Al_2(SO_4)_3$	8–10	16	200 rpm, 1 min	40 rpm, 15 min	20	—	63	34
FD-PSAF	2	10	120 rpm, 2 min	60 rpm, 7 min	20	99.7	—	35
PFS	2	13	120 rpm, 2 min	60 rpm, 7 min	20	98	—	35
PSFCL	5	30 (ml L^{-1})	200 rpm, 2 min	60 rpm, 5 min	30	97.5	95.1	The present study

[a] PFASiC, polyaluminium ferric silicate chloride; PAC, polyaluminium chloride; FD-PSAF, polysilicate aluminum ferric from foundry dust; PFS, polymerized ferrous sulfate; PSFCL, polysilicate ferric calcium lanthanum; TP, total phosphorus; TF, total fluoride.

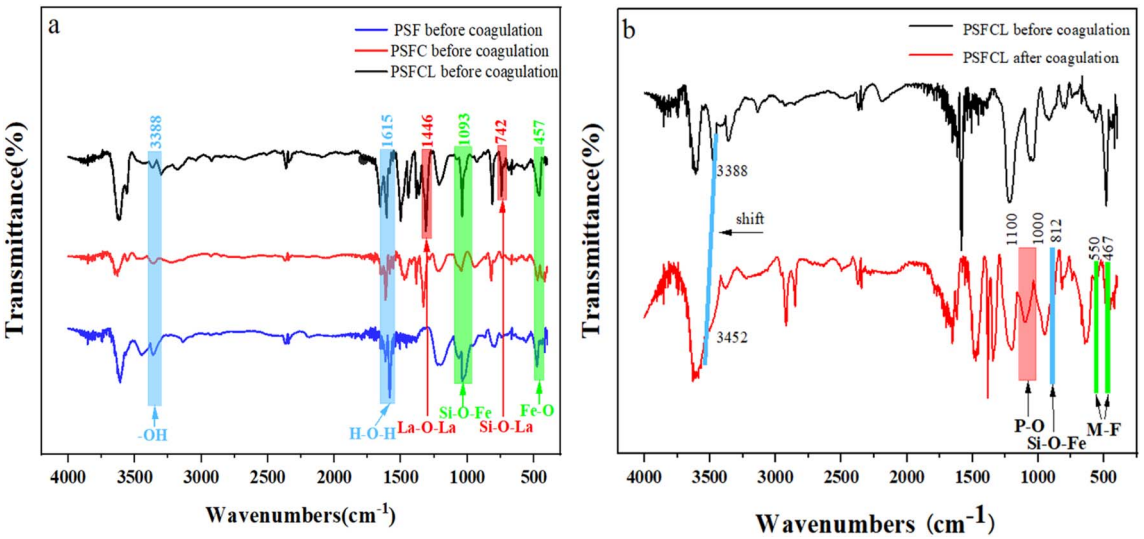

Fig. 5 (a) FT-IR spectra of three flocculants before coagulation; (b) FT-IR spectra of PSFCL flocculants before and after coagulation.

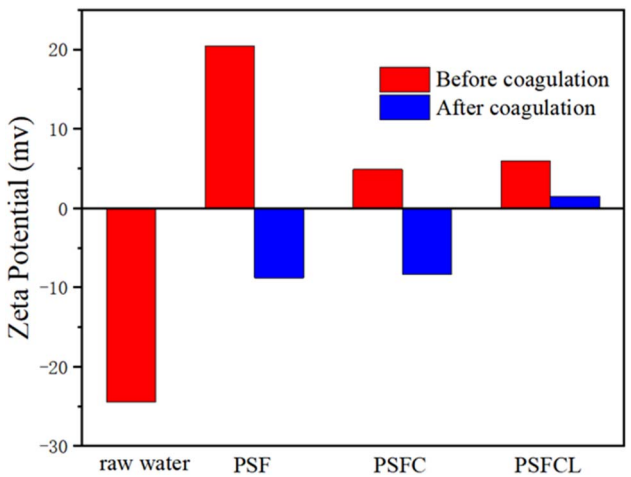

Fig. 6 Zeta potential of raw water, PSF, PSFC, PSFCL before and after coagulation.

According to previous studies, the ideal zeta potential value of a flocculant during the coagulation process was zero. Under this condition, the unstable-state particles within the water body were more conductive to agglomerate and subsequently achieve a good coagulation performance.[40] The zeta potential of PSF, PSFC and PSFCL after coagulation process was −8.82 mV, −8.4 mV, and 1.48 mV, respectively. Apparently, PSFCL had the best coagulation performance due to the lowest absolute zeta potential value, which corresponded to the results of previous coagulation experiments.

3.4.3 XPS analysis. X-ray photoelectron spectroscopy (XPS) analysis was displayed to determine the chemical constitution of synthesized flocculants surfaces before and after coagulation, as shown in Fig. 7. According to the wide scan XPS spectrum shown in Fig. 7a, the presence of La, Fe, Ca, Cl was consistent with the results of FT-IR. In Fig. S4a and b,† the existence of P 2p located at 133.4 eV and F 1s located at 685 eV demonstrated a successful coagulation process towards phosphorus and fluoride.[41] The spectrum of O 1s before and after coagulation could be deconvoluted into three components, as shown in Fig. 7b and c. Furthermore, three overlapped peaks corresponded to M–O (M = Fe, Ca, La, 530.53 eV), –OH (532.33 eV), H_2O (533.72 eV), respectively.[42] After coagulation, the area ratio of –OH decreased from 62% to 47%, indicating that the fluoride could bond with the flocculant through ligand exchange.[43] The spectrum of M–O shifted to a higher binding energy from 530.53 eV to 531.17 eV, as shown in Fig. 7c, which was possibly relevant to the generation of M–O–P and M–O–F inner–sphere complex through ligand exchange.[44,45] Moreover, the spectrum of La $3d_{3/2}$ and La $3d_{5/2}$ also shifted to a higher binding energy after coagulation, as shown in Fig. 7d and e. The result implied the formation of $LaPO_4$ and LaF. This proved that the surface precipitation also participated in the coagulation process.[46]

Finally, the possible mechanism schematic diagram of flocculation over PSFCL was shown in Fig. 8. The yellow phosphorus wastewater was negative in the analysis of zeta potential. After adding the positively charged composite flocculants PSFCL, it could bond with the colloid particles *via* charge neutralization and subsequently accelerate the formation of small flocs. PSFCL was a macromolecular substance due to the polymerization of polysilicic acid. This could consequently enhance the molecular weight of the composite and generate a strong bridging effect. PSFCL could also form a net-shaped structure within the water body, which could effectively capture the small flocs, leading to larger flocs and compact aggregates. Moreover, during the coagulation process, the loading positively charged metal ions could interact with phosphorus and fluoride ions through complexation, ligand exchange and co-precipitation process. As a whole, charge neutralization, bridging effect and ligand exchange were the main flocculation mechanisms.

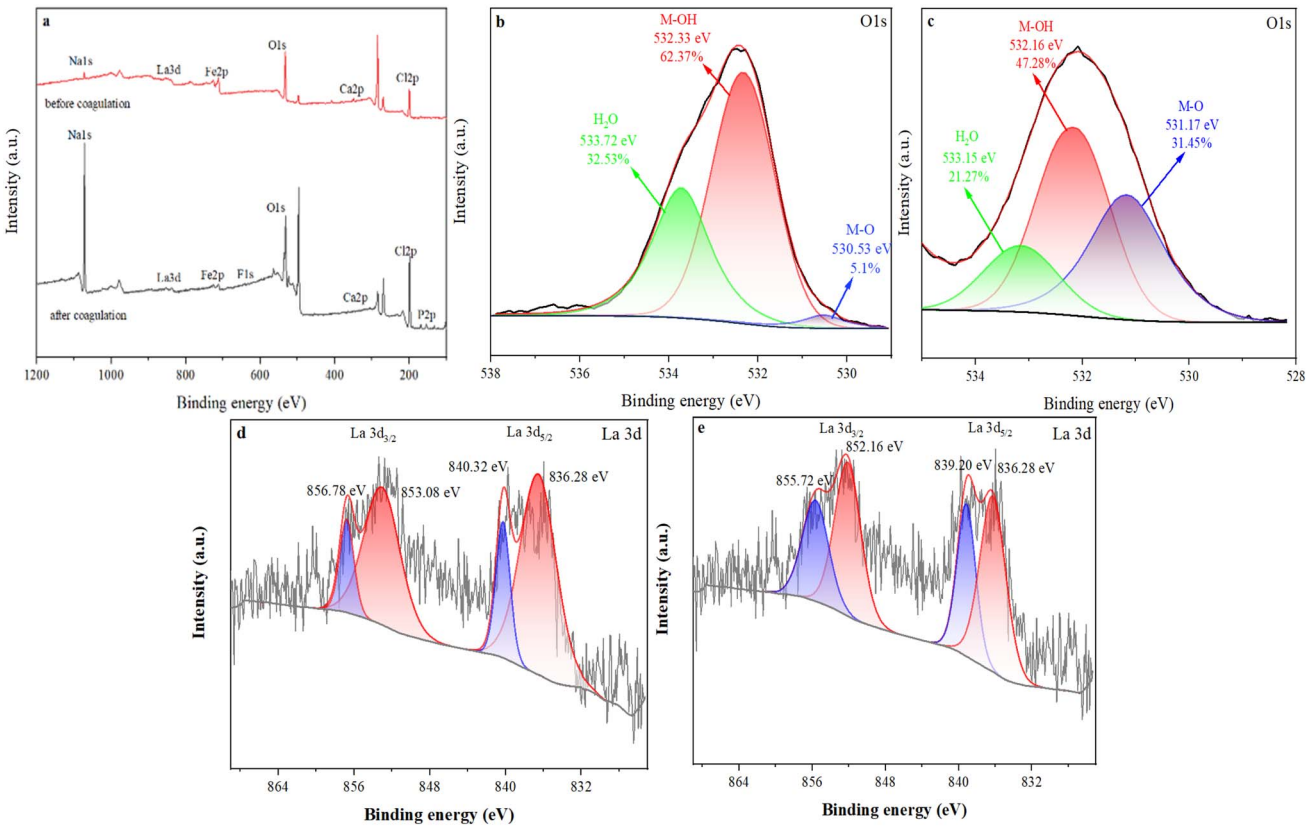

Fig. 7 (a) Wide XPS spectra of PSFCL before and after coagulation; (b) O 1s spectra of PSFCL before coagulation; (c) O 1s spectra of PSFCL after coagulation; (d) La 3d spectra of PSFCL before coagulation; (e) La 3d spectra of PSFCL after coagulation.

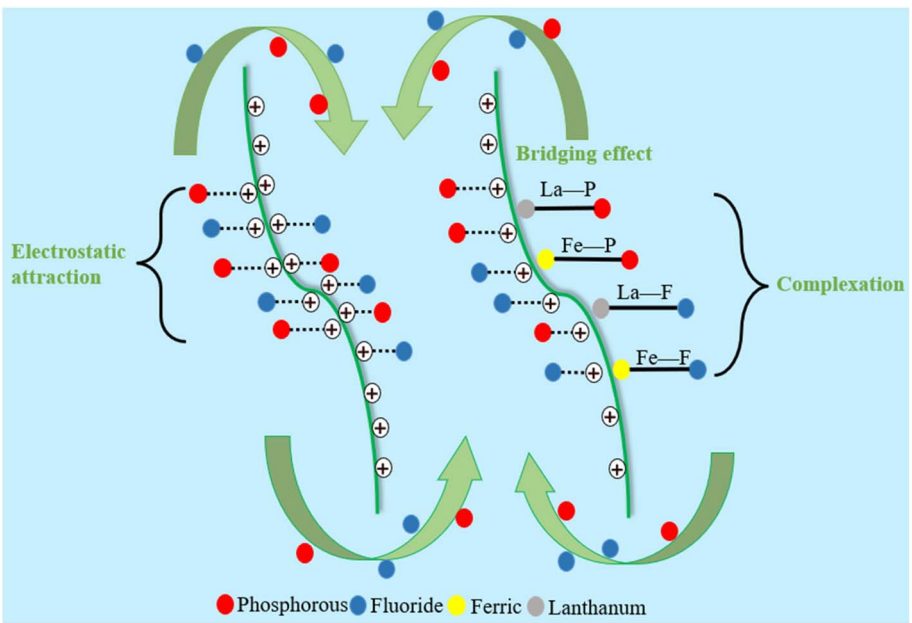

Fig. 8 Schematic mechanism of phosphorus and fluoride flocculation on PSFCL.

4. Conclusion

In this study, a polysilicate-ferric-calcium-lanthanum flocculant (PSFCL) was successfully prepared through co-polymerization method and employed to investigate its performance for yellow phosphorus wastewater treatment. The results shown that PSFCL possessed a better coagulation performance, and the removal efficiency towards phosphorus and fluoride was

95% and 87%, respectively, compared with PSF and PSFC. The flocculation conditions were set up by single-factor variable tests. The optimum conditions for removal of phosphorus and fluoride were confirmed, namely, the dosage was 6 ml L^{-1}, the sedimentation time was 30 min, the pH for flocculation was 5, the agitation time was less than 24 h, and the La/Si molar ratio was 0.3. The results from XPS and FTIR demonstrated that charge neutralization, bridging effect, ligand exchange and complexation existed in the flocculation process. In summary, the current work not only provided a new design for composite flocculants, but also exhibited an important significance in the optimization and future practical application for wastewater treatment.

Data availability

The data supporting this article have been included as part of the ESI.†

Conflicts of interest

There are no conflicts to declare.

Acknowledgements

The authors would like to acknowledge the financial support from Yunnan Major Scientific and Technological Projects (Grant No. 202202AG050001-5).

References

1 K. Y. Koh, S. Zhang and J. Paul Chen, Hydrothermally synthesized lanthanum carbonate nanorod for adsorption of phosphorus: material synthesis and optimization, and demonstration of excellent performance, *Chem. Eng. J.*, 2020, **380**, 122153.
2 M. Chaudhary and A. Maiti, Defluorination by highly efficient calcium hydroxide nanorods from synthetic and industrial wastewater, *Colloids Surf., A*, 2019, **561**, 79–88.
3 T. Robshaw, S. Tukra, D. B. Hammond, G. J. Leggett and M. D. Ogden, Highly efficient fluoride extraction from simulant leachate of spent potlining *via* La-loaded chelating resin. An equilibrium study, *J. Hazard. Mater.*, 2019, **361**, 200–209.
4 W. X. Gong, J. H. Qu, R. P. Liu and H. C. Lan, Effect of aluminum fluoride complexation on fluoride removal by coagulation, *Colloids Surf., A*, 2012, **395**, 88–93.
5 S. Raghav and D. Kumar, Comparative kinetics and thermodynamic studies of fluoride adsorption by two novel synthesized biopolymer composites, *Carbohydr. Polym.*, 2019, **203**, 430–440.
6 B. Rajasekhar, U. Venkateshwaran, N. Durairaj, G. Divyapriya, I. M. Nambi and A. Joseph, Comprehensive treatment of urban wastewaters using electrochemical advanced oxidation process, *J. Environ. Manage.*, 2020, **266**, 110469.
7 H. Zhang, Z. Zhang, K. Jiang, Z. Li, K. Zhang, J. Ma and Y. Qian, Salt effect on MUCT system performance of nitrogen and phosphorus removal, *Green Energy Environ.*, 2021, **6**(5), 670–677.
8 W. J. Xia, L. X. Guo, L. Q. Yu, Q. Zhang, J. R. Xiong, X. Y. Zhu, X. C. Wang, B. C. Huang and R. C. Jin, Phosphorus removal from diluted wastewaters using a La/C nanocomposite-doped membrane with adsorption-filtration dual functions, *Chem. Eng. J.*, 2021, **405**, 126924.
9 C. Y. Teh, P. M. Budiman, K. P. Y. Shak and T. Y. Wu, Recent Advancement of Coagulation–Flocculation and Its Application in Wastewater Treatment, *Ind. Eng. Chem. Res.*, 2016, **55**(16), 4363–4389.
10 X. Yu, C. Wei, H. Wu, Z. Jiang and R. Xu, Improvement of biodegradability for coking wastewater by selective adsorption of hydrophobic organic pollutants, *Sep. Purif. Technol.*, 2015, **151**, 23–30.
11 T. Sun, C. H. Sun, G. L. Zhu, X. J. Miao, C. C. Wu, S. B. Lv and W. J. Li, Preparation and coagulation performance of poly-ferric-aluminum-silicate-sulfate from fly ash, *Desalination*, 2011, **268**(1–3), 270–275.
12 Z. Zhang, H. Zheng, Y. Sun, C. Zhao, Y. Zhou, X. Tang and C. Zhao, A combined process of chemical precipitation and flocculation for treating phosphating wastewater, *Desalin. Water Treat.*, 2016, **57**(53), 25520–25531.
13 B. Macherzyński, M. Wszelaka-Rylik, M. Włodarczyk-Makuła, M. Osiak, A. Pietrzak, B. Bień and A. Poniatowska, Comparative efficiency of phosphorus removal from supernatants by coagulation process, *Desalin. Water Treat.*, 2023, **301**, 209–215.
14 N. Ozairi, S. A. Mousavi, M. T. Samadi, A. Seidmohammadi and D. Nayeri, Removal of fluoride from water using coagulation–flocculation process: a comparative study, *Desalin. Water Treat.*, 2020, **180**, 265–270.
15 C. Zhao, J. Zhang, Z. Luan, X. Peng and X. Ren, Preparation of high concentration polyaluminum chloride with high content of Alb or Alc, *J. Environ. Sci.*, 2009, **21**(10), 1342–1346.
16 Z. P. Xing and D. Z. Sun, Treatment of antibiotic fermentation wastewater by combined polyferric sulfate coagulation, fenton and sedimentation process, *J. Hazard. Mater.*, 2009, **168**(2–3), 1264–1268.
17 G. Lei, J. Ma, X. Guan, A. Song and Y. Cui, Effect of basicity on coagulation performance of polyferric chloride applied in eutrophicated raw water, *Desalination*, 2009, **247**(1–3), 518–529.
18 A. Campbell, D. Hamai and S. C. Bondy, Differential toxicity of aluminum salts in human cell lines of neural origin: implications for neurodegeneration, *Neurotoxicology*, 2001, **22**(1), 63–71.
19 R. F. Packham, Some studies of the coagulation of dispersed clays with hydrolyzing salts, *J. Colloid Sci.*, 1965, **20**(1), 81–92.
20 Z. M. Liu, Y. M. Sang, Z. G. Tong, Q. H. Wang and T. C. Sun, Decolourization performance and mechanism of leachate secondary effluent using poly-aluminium(III)–magnesium(II) sulphate, *Water Environ. J.*, 2012, **26**(1), 85–93.
21 Y. Liu, J. Ma, L. Lian, X. Wang, H. Zhang, W. Gao and D. Lou, Flocculation performance of alginate grafted polysilicate

aluminum calcium in drinking water treatment, *Process Saf. Environ. Prot.*, 2021, **155**, 287–294.

22 L. Wu, Y. Gao, X. Xu, J. Deng and H. Liu, Excellent coagulation performance of polysilicate aluminum ferric for treating oily wastewater from Daqing gasfield: responses to polymer properties and coagulation mechanism, *J. Environ. Manage.*, 2024, **356**, 120642.

23 Q. Lin, H. Peng, S. Zhong and J. Xiang, Synthesis, characterization, and secondary sludge dewatering performance of a novel combined silicon–aluminum–iron–starch flocculant, *J. Hazard. Mater.*, 2015, **285**, 199–206.

24 W. Chen, H. Zheng, J. Zhai, Y. Wang, W. Xue, X. Tang, Z. Zhang and Y. Sun, Characterization and coagulation–flocculation performance of a composite coagulant: poly-ferric-aluminum-silicate-sulfate, *Desalin. Water Treat.*, 2015, **56**(7), 1776–1786.

25 J. Yi, Z. Chen, D. Xu, D. Wu and A. Howard, Preparation of a coagulant of polysilicate aluminum ferric from foundry dust and its coagulation performance in treatment of swine wastewater, *J. Cleaner Prod.*, 2024, **434**, 140400.

26 Y. Sun, C. Zhu, H. Zheng, W. Sun, Y. Xu, X. Xiao, Z. You and C. Liu, Characterization and coagulation behavior of polymeric aluminum ferric silicate for high-concentration oily wastewater treatment, *Chem. Eng. Res. Des.*, 2017, **119**, 23–32.

27 J. Li, J. Li, X. Liu, Z. Du and F. Cheng, Effect of silicon content on preparation and coagulation performance of poly-silicic-metal coagulants derived from coal gangue for coking wastewater treatment, *Sep. Purif. Technol.*, 2018, **202**, 149–156.

28 K. You, W. Yang, P. Song, L. Fan, S. Xu, B. Li and L. Feng, Lanthanum-modified magnetic oyster shell and its use for enhancing phosphate removal from water, *Colloids Surf., A*, 2022, **633**, 127897.

29 C. Liu, B. Gao, S. Wang, K. Guo, X. Shen, Q. Yue and X. Xu, Synthesis, characterization and flocculation performance of a novel sodium alginate-based flocculant, *Carbohydr. Polym.*, 2020, **248**, 116790.

30 T. Krahnstöver and T. Wintgens, Optimizing the flocculation of powdered activated carbon in wastewater treatment by dosing iron salt in single- and two-stage processes, *J. Water Process. Eng.*, 2017, **20**, 130–137.

31 T. Kim, The effects of polyaluminum chloride on the mechanical and microstructural properties of alkali-activated slag cement paste, *Cem. Concr. Compos.*, 2019, **96**, 46–54.

32 T. Chen, M. Niu, X. Wang, W. Wei, J. Liu and Y. Xie, Synthesis and characterization of poly-aluminum silicate sulphate (PASS) for ultra-low density fiberboard (ULDF), *RSC Adv.*, 2015, **5**(113), 93187–93193.

33 X. Niu, X. Li, J. Zhao, Y. Ren and Y. Yang, Preparation and coagulation efficiency of polyaluminium ferric silicate chloride composite coagulant from wastewater of high-purity graphite production, *J. Environ. Sci.*, 2011, **23**(7), 1122–1128.

34 Y. Gan, X. Wang, L. Zhang, B. Wu, G. Zhang and S. Zhang, Coagulation removal of fluoride by zirconium tetrachloride: performance evaluation and mechanism analysis, *Chemosphere*, 2019, **218**, 860–868.

35 J. Yi, Z. Chen, D. Xu, D. Wu and A. Howard, Preparation of a coagulant of polysilicate aluminum ferric from foundry dust and its coagulation performance in treatment of swine wastewater, *J. Cleaner Prod.*, 2024, **434**, 140400.

36 B. Zhang, Z. Chang, J. Li, X. Li, Y. Kan and Z. Gao, Effect of kaolin content on the performances of kaolin-hybridized soybean meal-based adhesives for wood composites, *Composites, Part B*, 2019, **173**, 106919.

37 M. Li, S. Kuang, Y. Kang, H. Ma, J. Dong and Z. Guo, Recent advances in application of iron-manganese oxide nanomaterials for removal of heavy metals in the aquatic environment, *Sci. Total Environ.*, 2022, **819**, 153157.

38 B. Zhang, L. Xu, Z. Zhao, S. Peng, C. Yu, X. Zhang, Y. Zong and D. Wu, Enhanced phosphate removal by nano-lanthanum hydroxide embedded silica aerogel composites: superior performance and insights into specific adsorption mechanism, *Sep. Purif. Technol.*, 2022, **285**, 120365.

39 P. K. Raul, R. R. Devi, I. M. Umlong, S. Banerjee, L. Singh and M. Purkait, Removal of Fluoride from Water Using Iron Oxide-Hydroxide Nanoparticles, *J. Nanosci. Nanotechnol.*, 2012, **12**(5), 3922–3930.

40 G. P. Lam, E. K. Zegeye, M. H. Vermuë, D. M. M. Kleinegris, M. H. M. Eppink, R. H. Wijffels and G. Olivieri, Dosage effect of cationic polymers on the flocculation efficiency of the marine microalga Neochloris oleoabundans, *Bioresour. Technol.*, 2015, **198**, 797–802.

41 J. He, K. Zhang, S. Wu, X. Cai, K. Chen, Y. Li, B. Sun, Y. Jia, F. Meng, Z. Jin, L. Kong and J. Liu, Performance of novel hydroxyapatite nanowires in treatment of fluoride contaminated water, *J. Hazard. Mater.*, 2016, **303**, 119–130.

42 L. Chen, K. S. Zhang, J. Y. He, W. H. Xu, X. J. Huang and J. H. Liu, Enhanced fluoride removal from water by sulfate-doped hydroxyapatite hierarchical hollow microspheres, *Chem. Eng. J.*, 2016, **285**, 616–624.

43 M. Yi, K. Wang, H. Wei, D. Wei, X. Wei, B. Wei, L. Shao, T. Fujita and X. Cui, Efficient preparation of red mud-based geopolymer microspheres (RM@GMs) and adsorption of fluoride ions in wastewater, *J. Hazard. Mater.*, 2023, **442**, 130027.

44 Y. Jia, B. S. Zhu, K. S. Zhang, Z. Jin, B. Sun, T. Luo, X. Y. Yu, L. T. Kong and J. H. Liu, Porous 2-line ferrihydrite/bayerite composites (LFBC): fluoride removal performance and mechanism, *Chem. Eng. J.*, 2015, **268**, 325–336.

45 X. Wu, Y. Zhang, X. Dou, B. Zhao and M. Yang, Fluoride adsorption on an Fe–Al–Ce trimetal hydrous oxide: characterization of adsorption sites and adsorbed fluorine complex species, *Chem. Eng. J.*, 2013, **223**, 364–370.

46 P. Koilraj and K. Sasaki, Selective removal of phosphate using La-porous carbon composites from aqueous solutions: batch and column studies, *Chem. Eng. J.*, 2017, **317**, 1059–1068.